Journal of The Electrochemical Society, **150** (11) A1498-A1502 (2003)
0013-4651/2003/150(11)/A1498/5/$7.00 © The Electrochemical Society, Inc.

Significance of the Tetrahedral A Site on the Electrochemical Performance of Substituted $Li_{1.05}M_{0.05}Mn_{1.90}O_4$ Spinel Electrodes (M = Li, Mg, Zn, Al) in Lithium Cells

J.-S. Kim,* J. T. Vaughey,* C. S. Johnson,* and M. M. Thackeray*,z

Electrochemical Technology Program, Chemical Technology Division, Argonne National Laboratory, Argonne, Illinois 60439, USA

The electrochemical performance of substituted $Li_{1.05}M_{0.05}Mn_{1.90}O_4$ spinel electrodes (M = Li, Mg, Zn, Al) in lithium cells has been studied as a function of the oxidation states of the M and Mn ions in the parent electrode, and the occupancy of the tetrahedral A sites by the Li and the M ions. At 5% substitution of manganese, neutron diffraction analyses show that the M ions reside at the A sites of the $A[B_2]O_4$ spinel structure. The electrochemical data showed that at 50°C the rate of capacity fade can be correlated with the M-ion occupancy of the A sites. A possible explanation for this phenomenon is provided.
 [DOI: 10.1149/1.1614798]

Manuscript submitted January 23, 2003; revised manuscript received April 4, 2003. This was Paper 128 presented at the Salt Lake City, Utah, Meeting of the Society, October 20-25, 2002. Available electronically September 22, 2003.

The discovery about twenty years ago that the $[B_2]X_4$ framework of an $A[B_2]X_4$ spinel remained intact during the electrochemical insertion and extraction of lithium has led to intense investigations of spinel compounds as possible insertion electrodes for lithium batteries.[1-3] Of particular significance has been the family of lithium spinels $Li[B_2]O_4$ (B = Mn, Ti, Li), such as $LiMn_2O_4$ and $Li_4Ti_5O_{12}$ ($Li[Li_{0.33}Ti_{1.67}]O_4$ in which the $[B_2]O_4$ spinel framework provides a three-dimensional (3-D) interstitial space for lithium.[4,5] The manganese spinel $LiMn_2O_4$ received early attention because it provides approximately 4 V against lithium over the compositional range $Li_{1-x}Mn_2O_4$ ($0 < x \leq 1$) and is therefore a possible alternative to the $LiCoO_2$ electrode in conventional Li-ion cells.[6,7] Despite the structural advantage of $Li[Mn_2]O_4$ electrodes, $Li_xC_6/Li_{1-x}Mn_2O_4$, lithium-ion cells suffer from capacity fade, particularly at elevated temperatures (>40°C). The capacity fade has been attributed to the dissolution of manganese from the spinel structure (as Mn^{2+}) by acid attack, for example, by HF generated by hydrolysis of a fluorinated electrolyte salt such as $LiPF_6$, according to the disproportionation reaction

$$2Mn^{3+}_{(solid)} \rightarrow Mn^{4+}_{(solid)} + Mn^{2+}_{(solution)} \quad [1]$$

Several strategies have been adopted to counter the acid attack and to suppress the dissolution of the spinel electrode

1. Substitute some of the Mn^{3+} ions in $LiMn_2O_4$ by monovalent, divalent, or trivalent cations such as Li^+, Mg^{2+}, Zn^{2+}, and Al^{3+} to increase the Mn^{4+} ion content in the initial spinel electrode,[8-13]
2. Coat the spinel particles,[14,15] or
3. Replace $LiPF_6$ with a nonfluorinated salt such as lithium bis(oxalato)borate, $LiB(C_2O_4)_2$ ("LiBOB")[16] to reduce the acidity of the electrolyte.[17]

In this paper we explore the first strategy. We report electrochemical data obtained from various spinel electrodes with 5% substitution of the manganese ions, $Li_{1.05}M_{0.05}Mn_{1.90}O_4$ (M = Li, Mg, Zn, Al), in lithium cells at room temperature and at 50°C as a function of 1) the oxidation state of the substituting M ion, and 2) the oxidation state of the Mn ions in the parent electrode. Although it is well known that these substituted spinels can provide superior cycling stability compared to $LiMn_2O_4$, to the best of our knowledge this is the first time that a systematic structural study of a series of substituted spinel electrodes has been undertaken by neutron diffraction and correlated with the electrochemical performance of the electrodes. We use these data to make a hypothesis that the occupation of tetrahedral sites by the substituting ions, particularly Al, at the surface of the spinel structure retards Mn dissolution.

Experimental

Samples of substituted spinel compounds $Li_{1.05}M_{0.05}Mn_{1.90}O_4$ (M = Li, Mg, Al, Zn,) were synthesized by first dissolving manganese acetate and the appropriate metal acetates, $M(CH_3CO_2)_n \cdot xH_2O$, in distilled water in the required amounts, and then by mixing the resulting solution with glycolic acid while stirring continuously. Thereafter, ammonium hydroxide was added slowly to the solution to control the pH at ~8. The solution was heated at 70°C to evaporate the water to yield a transparent gel that was subsequently decomposed at 400°C for 5 h in air. The resulting powder was pressed into pellets and heated at 800°C for an additional 5 h in air to obtain the final spinel product.

Electrodes were fabricated by intimately mixing 85 wt % $Li_{1.05}M_{0.05}Mn_{1.90}O_4$ powder, 8 wt % polyvinylidene difluoride (PVDF) binder (Kynar, Elf-Autochem), and 7 wt % acetylene black (Cabot) in a 1-methyl-2-pyrrolidinone (NMP) solvent (Aldrich, 99+%). The mixed slurry was cast onto aluminum foil and dried at 75°C for 3-5 h. The cast electrode laminates were dried further at 70°C under vacuum overnight. Disk electrodes with an area of 1.6 cm^2 were punched out from the laminates. Electrochemical evaluations of the spinel electrodes were performed with coin-type cells (size 2032, Hohsen Corporation) having a lithium foil (FMC Corporation) counter electrode, a polypropylene separator (Celgard), and an electrolyte consisting of a 1 M $LiPF_6$ solution with a 1:1 ethylene carbonate:diethylcarbonate solvent mixture (Merck). Cells were constructed inside a helium-filled glove box (<5 ppm, H_2O and O_2). Galvanostatically controlled cycling of the lithium cells was carried out using a Maccor Series 2000 battery tester at a current rate of 0.1 mA/cm^2.

Time-of-flight neutron diffraction data were collected on the substituted spinel samples, contained in a vanadium can, using the special-environment powder diffractometer at the Intense Pulse Neutron Source (IPNS) at Argonne National Laboratory. The diffraction data were collected at room temperature. Structures were refined by a Rietveld profile fitting procedure with the GSAS suite of programs[18] using the *d* spacing range 0.67-3.00 Å from a ±145° 2θ data bank.

Results and Discussion

The significance of the tetrahedral A site in substituted spinel electrodes.—The [110] projection of the standard $Li_{8a}[Mn_2]_{16d}O_4$ spinel structure is shown in Fig. 1; it has cubic symmetry $Fd3m$. This figure shows the MnO_6 octahedra (shaded) in which the Mn ions occupied 16d sites and the positions of the lithium ions in the

* Electrochemical Society Active Member.
z E-mail: thackeray@cmt.anl.gov

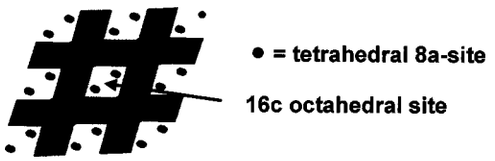

Figure 1. A [110] projection of the $LiMn_2O_4$ spinel structure showing the MnO_6 octahedra (shaded, Mn in 16d sites) and the positions of the tetrahedral 8a (A) sites and octahedral 16c sites for Li^+-ion diffusion during electrochemical charge and discharge.

tetrahedral 8a (A) sites; it also shows the positions of neighboring face-shared, interstitial octahedral (16c) sites. The 3-D 8a-16c-8a-16c-network provides an energetically favorable pathway for the rapid diffusion of lithium in and out of the structure during discharge and charge, respectively. If $LiMn_2O_4$ is used as an electrode in a lithium-ion cell then, in principle, it is possible to electrochemically extract all the lithium to yield the fully delithiated, defect spinel structure λ-MnO_2. In substituted spinels, taking the lithium-substituted spinels $Li_{1+x}Mn_{2-x}O_4$ as an example, lithium extraction must of necessity leave some lithium within the interstitial space at the top of charge, *i.e.*, when the average oxidation state of the manganese ions reaches 4.0.[8] For example, in $Li_{1.1}Mn_{1.9}O_4$ (in spinel notation, $Li[Mn_{1.9}Li_{0.1}]O_4$), the additional 0.1 Li^+ ions in the structure raise the average oxidation state of the manganese ions to 3.63 from 3.50 in the parent, unsubstituted spinel $LiMn_2O_4$. Therefore, only 0.7 Li^+ ions can be extracted from $Li_{1.1}Mn_{1.9}O_4$ as opposed to the 1.0 Li^+ ions that can be extracted from $LiMn_2O_4$, thereby lowering the theoretical capacity from 148 mAh/g for $LiMn_2O_4$ to 107 mAh/g for $Li_{1.1}Mn_{1.9}O_4$. The composition of a fully delithiated $Li_{1.1-x}Mn_{1.9}O_4$ electrode at the top of charge is $Li_{0.4}Mn_{1.9}O_4$ ($x = 0.7$); at this composition, 0.3 Li^+ ions must remain in the tetrahedral A sites of the spinel structure, assuming that 0.1 Li^+ ions remain on the octahedral B (16d) sites in the original electrode structure.

As shown in Reaction 1, manganese dissolves from the spinel structure as a divalent ion. Mn^{2+} is a d^5 ion with no crystal field stabilization energy. Therefore, Mn^{2+} ions can readily occupy both tetrahedral and octahedral sites-for example, in Mn_3O_4 (a normal spinel), Mn^{2+} ions occupy the tetrahedral sites and Mn^{3+} ions the octahedral sites, whereas in rocksalt MnO, all the Mn^{2+} ions occupy octahedral sites. It is therefore tempting to speculate that the manganese ions should pass through tetrahedral sites at the surface of the spinel electrode particles during the dissolution process, as has already been proposed in a previous discussion of the acid treatment of $LiMn_2O_4$.[19] If that is true, then it stands to reason that stabilized spinel electrodes $LiM_xMn_{2-x}O_4$ that always contain some residual M ions in the tetrahedral A-sites of the spinel structure, *i.e.*, within the 8a-16c-8a-16c-diffusion pathway, should retard the dissolution process. This hypothesis is consistent with the electrochemical behavior and structural properties of $Li_{1+x}Mn_{2-x}O_4$ spinel electrodes such as $Li_{1.03}Mn_{1.97}O_4$.[8] Such a mechanism is also consistent with *ab initio* calculations for the transformation of delithiated layered Li_xMnO_2 to the spinel structure that predict the migration of divalent manganese through intermediate tetrahedral sites.[20]

With the above viewpoint in mind, we embarked on a study of spinel electrodes in which 2.5% of the manganese ions were substituted by lithium and 2.5% by M cations that could have a stronger affinity for tetrahedral coordination than lithium, such as Zn and Al. For example, it has already been demonstrated that in Zn-substituted $LiMn_{2-x}Zn_xO_4$ spinels, zinc substitutes for lithium on the tetrahedral sites.[21] In the lithium aluminate spinel, the cation distribution is $Al[Li_{0.5}Al_{1.5}]O_4$, and in the mineral spinel $Mg[Al_2]O_4$, Mg occupies the tetrahedral sites in preference to Al;[22] therefore, by implication, Mg may show a stronger preference for the tetrahedral sites than lithium in $LiMn_{2-x}Mg_xO_4$. Several other neutron diffraction studies of substituted $LiM_xMn_{2-x}O_4$ spinels have already been conducted; for example, cobalt and iron substitution occurs on tetrahedral sites,[23] nickel substitution occurs on octahedral sites,[24] and gallium substitution takes place predominantly on octahedral sites.[25] A recent study of $LiAl_xMn_{2-x}O_4$ samples by neutron diffraction has shown that aluminum substitutes for manganese on the octahedral sites for $x \geqslant 0.1$, but that phase separation occurs for $x \geqslant 0.3$.[26]

Table I. Neutron scattering lengths for various elements.

Element	Scattering length ($\times 10^{-12}$ cm)
Lithium	−0.203
Manganese	−0.373
Aluminum	+0.3449
Magnesium	+0.5375
Zinc	+0.5680
Oxygen	+0.5805

Neutron diffraction analysis of $Li_{1.05}M_{0.05}Mn_{1.90}O_4$ structures ($M = Mg, Zn, Al$).—A major advantage of neutron diffraction is that, unlike X-ray diffraction, it can be used to determine the positions of light atoms such as hydrogen and lithium within crystallographic structures because it is the atomic nuclei rather than the extra-nuclear electrons that are responsible for the scattering of the neutron beam. Furthermore, the strong contrast in the neutron scattering power of elements that have small differences in atomic number makes it possible in certain instances to model the structures of materials far more accurately than with X-rays. Table I shows the scattering lengths of the atoms in the substituted spinel electrodes of this investigation. Both lithium and manganese have negative scattering lengths, that of manganese (-0.373×10^{-12} cm) is almost twice as large as lithium (-0.203×10^{-12} cm). However, all the M ions, Mg, Zn, Al, in the substituted $Li_{1.05}M_{0.05}Mn_{1.90}O_4$ electrodes have positive scattering lengths that contrast strongly with lithium. Therefore, it stands to reason that neutron diffraction should provide an excellent technique for determining the extent to which the M ions substitute for lithium on the tetrahedral A site of the spinel structure at low M concentrations.

The structural refinements of the three $Li_{1.05}M_{0.05}Mn_{1.90}O_4$ compounds (M = Mg, Zn, Al) yielded similar results. Therefore, the neutron diffraction profile and structural parameters for only one compound, $Li_{1.05}Al_{0.05}Mn_{1.9}O_4$, are provided in full. The observed, calculated and difference profiles for $Li_{1.05}Al_{0.05}Mn_{1.9}O_4$ are provided in Fig. 2; the crystallographic parameters of the refined structure are listed in Table II. For this refinement, it was assumed that

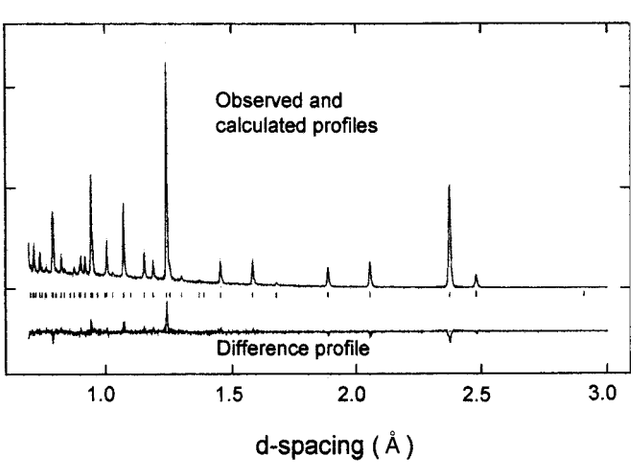

Figure 2. The powder neutron diffraction profile of $LiAl_{0.05}Mn_{1.95}O_4$.

Table II. Structural parameters of $Li_{1.05}Al_{0.05}Mn_{1.90}O_4$.[a]

Atom	*x*	*y*	*z*	$B(Å^2)$	Occupancy
Li	0.125	0.125	0.125	0.11(4)	0.949(7)
Al	0.125	0.125	0.125	0.11(4)	0.051(7)
Mn	0.5	0.5	0.5	0.11(4)	0.975(4)
Li	0.5	0.5	0.5	0.11(4)	0.025(4)
O	0.2634(1)	0.2634(1)	0.2634(1)	0.40(3)	1

[a] Space group $Fd3m$; $a = 8.2246(1)$Å.

the spinel structure was stoichiometric, *i.e.*, there were no oxygen defects. The oxygen occupancy was therefore fixed at 1.0 to "lock" the spinel structure during the refinement process. The *x* coordinate and isotropic temperature factor of the oxygen ions were varied independently. The atomic coordinates of the lithium, manganese, and aluminum ions were held constant by virtue of crystallographic symmetry. These ions were assigned the same variable isotropic temperature factor. The manganese ions were constrained to the octahedral B sites of the spinel structure (at 0.5, 0.5, 0.5), whereas the lithium and aluminum ions were permitted to occupy both the tetrahedral A sites (at 0.125, 0.125, 0.125) and the B sites; however, during the refinement, the total occupancy of the each of the A and B sites of these ions was constrained to 1. With this arrangement, the structural model that provided the best fit of experimental to calculated data showed that all of the aluminum was located on the tetrahedral A site. The refined Al occupancy of this site [0.051(7)] was in excellent agreement with the expected 5% value. All attempts to place the Al atoms on the B sites led to higher *R* factors. Refinement of the manganese and lithium on the octahedral B sites produced a manganese site occupancy of 0.975, slightly higher than the expected value of 0.950, implying that the diffraction data were not of sufficiently high quality to distinguish precisely the negatively scattering lithium atoms and manganese atoms on the B sites at a 5% substitution level.

The final refinement yielded a residual profile factor, R_p, of 8.5%. The refined lattice parameter, $a = 8.2246(1)$ Å, is lower than that of the standard spinel $LiMn_2O_4$ ($a = 8.2476$ Å), consistent with the trend shown by other substituted spinel compounds that have an average manganese oxidation state above 3.5,[8] and is comparable with $a = 8.2242(1)$ Å reported for $LiAl_{0.1}Mn_{1.9}O_4$ by Komaba *et al.*[26] However, our refinement showed a tetrahedral site preference for Al in a substituted spinel containing 2.5% Al and 2.5% excess Li, whereas at higher Al concentrations and in the absence of surplus Li, Komaba *et al.* provide evidence for Al at the octahedral sites.[26]

The refinement of the Mg- and Zn-substituted spinel structures provided results almost identical to those for the Al-substituted spinel, yielding lattice parameters of 8.2301(1) and 8.2308(1), A site occupancies of 0.05(1) and 0.10(2), and R_p values of 8.3 and 8.1, respectively. The slightly smaller lattice parameter of the Al-substituted spinel structure [$a = 8.2246(1)$ Å] compared to those of the Mg- and Zn-substituted spinel structures is consistent with the significantly smaller ionic radius of Al^{3+} ions in tetrahedral coordination (0.39 Å) compared to Li^+ (0.59 Å), Mg^{2+} (0.57 Å), and Zn^{2+} (0.60 Å).[27] Although the refinement of the zinc-substituted spinel yielded a slightly higher tetrahedral A site occupancy than expected, this result nevertheless clearly emphasized the stronger tetrahedral site preference of zinc over lithium, consistent with other neutron diffraction analyses of $LiMn_{2-x}Zn_xO_4$ spinel samples $0 < x \leq 0.5$,[21] which was the most important aspect of the structural analysis.

Electrochemical behavior of substituted spinel electrodes.—Cation substitution in $LiM_xMn_{2-x}O_4$ spinel electrodes lowers the electrochemical capacity relative to $LiMn_2O_4$, the extent of which depends not only on the degree of substitution but also on the valence of the substituting M ion. In general, the electrochemical capacity is most severely impacted when M is a monovalent ion, and less so for ions with increasing valence. For example, when M is selected from Li, Mg, Zn, and Al, the theoretical capacity of a $Li_{1.05}M_{0.05}Mn_{1.90}O_4$ electrode increases from 107 mAh/g for $M = Li^+$ to 121 mAh/g for Al^{3+}, which is consistent with the corresponding decrease in the average oxidation state of the Mn ions from 3.63 to 3.58 (Table III); by comparison, the capacity of an unsubstituted spinel $LiMn_2O_4$ electrode, in which the average manganese valence is 3.5, is 148 mAh/g.

Table III. Mn oxidation state and capacity of $Li_{1.05}M_{0.05}Mn_{1.90}O_4$ spinel electrodes (M = Li, Mg, Zn, Al).

Spinel composition	M ion	Average oxidation state of Mn ion	Electrode capacity (mAh/g)
$Li_{1.05}Li_{0.05}Mn_{1.90}O_4$	Li^{1+}	3.63	107
$Li_{1.05}Zn_{0.05}Mn_{1.90}O_4$	Li^{1+}/Zn^{2+}	3.60	112
$Li_{1.05}Mg_{0.05}Mn_{1.90}O_4$	Li^{1+}/Mg^{2+}	3.60	114
$Li_{1.05}Al_{0.05}Mn_{1.90}O_4$	Li^{1+}/Al^{3+}	3.58	121
$LiMn_2O_4$	-	3.50	148

The electrochemical charge/discharge profiles of a standard $Li/LiMn_2O_4$ cell cycled between 4.3 and 3.3 V is compared with the voltage profiles of $Li/Li_{1.05}M_{0.05}Mn_{1.90}O_4$ cells (M = Al, Zn) at room temperature in Fig. 3. During lithium extraction from $LiMn_2O_4$, a voltage step only ~130 mV in magnitude that occurs approximately halfway along the voltage curve has been attributed previously to a cubic-cubic transition, which is associated with an ordering of one-half of the lithium ions on the tetrahedral sites[28] and/or to electronic ordering of the manganese ions on the octahedral B sites[29] at the composition $Li_{0.5}Mn_2O_4$. Such ordering processes are crystallographically permissible for the ideal spinel composition, $Li[Mn_2]O_4$. However, substitution for Mn by the M ions in $Li_{1.05}M_{0.05}Mn_{1.90}O_4$ spinel electrodes must of necessity disrupt the long-range crystallographic order within the spinel structure; moreover, the presence of the substituted M ions on the tetrahedral sites must also significantly affect such a small and subtle transition. Indeed, it has now been well established that the transition in substituted spinel electrodes is not as clearly visible as it is in $Li_{1-x}Mn_2O_4$ electrodes,[8,30,31] this phenomenon is also clearly apparent in the voltage profiles of the $Li/Li_{1.05}M_{0.05}Mn_{1.90}O_4$ cells in Fig. 3, and is consistent with the recent data reported by Komaba *et al.* for $Li/LiAl_xMn_{2-x}O_4$ cells for $0 \leq x \leq 0.3$.[13] Our interpretation of this phenomenon is that the cubic-cubic transition is suppressed in

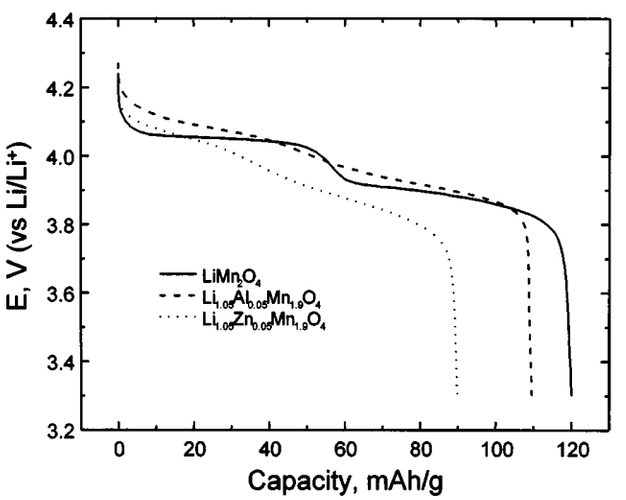

Figure 3. The electrochemical charge/discharge profiles recorded at room temperature of a standard $Li/LiMn_2O_4$ cell compared with a $Li/Li_{1.05}Al_{0.05}Mn_{1.9}O_4$ cell and a $Li/Li_{1.05}Zn_{0.05}Mn_{1.90}O_4$ cell.

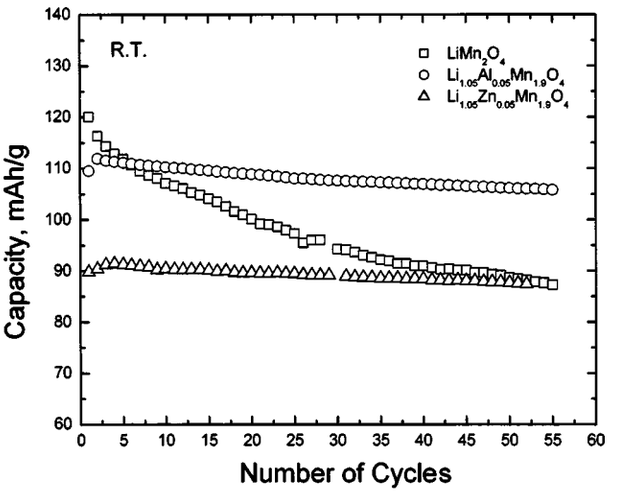

Figure 4. Capacity *vs.* cycle no. plots recorded at room temperature for substituted $Li_{1.05}M_{0.05}Mn_{1.90}O_4$ spinel electrodes (M = Al, Zn) compared with a standard $LiMn_2O_4$ electrode for cycles 1-55.

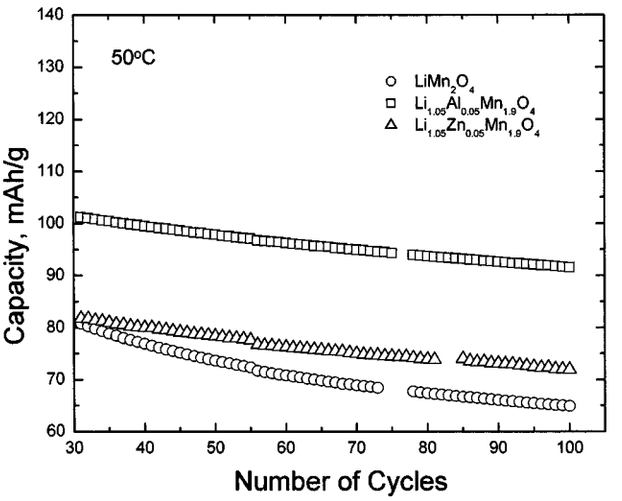

Figure 6. Capacity *vs.* cycle number plots recorded at 50°C for substituted $Li_{1.05}M_{0.05}Mn_{1.90}O_4$ spinel electrodes (M = Al, Zn) compared with a standard $LiMn_2O_4$ electrode for cycles 30-100.

substituted spinel electrodes with inhomogeneous and asymmetric structures; nevertheless, this interpretation does not rule out the possibility that the transition can occur locally in selected regions of the electrode structure when permitted by crystallographic symmetry.

Spinel electrode capacity *vs.* cycle number plots for various $Li/Li_{1.05}M_{0.05}Mn_{1.90}O_4$ cells are compared with a standard $Li/LiMn_2O_4$ cell at room temperature (55 cycles) and at 50°C (~30 cycles) in Fig. 4 and 5, respectively. The standard $LiMn_2O_4$ electrode lost capacity steadily at room temperature and more rapidly at 50°C, consistent with earlier reports.[32] By contrast, the rate of capacity loss of the substituted $Li_{1.05}M_{0.05}Mn_{1.90}O_4$ electrodes was significantly less, the amount of delivered capacity being proportional to the theoretical capacity as determined from the average oxidation state of the manganese ions in the parent electrode (Table III). Of particular significance to this study is that the relative rate of capacity fade of the all substituted electrodes is approximately the same, *i.e.*, the capacity *vs.* cycle number plots lie closely parallel to one another. Such a striking similarity appears to be more than a coincidence, and we attribute this phenomenon to the residual Li, Mg,

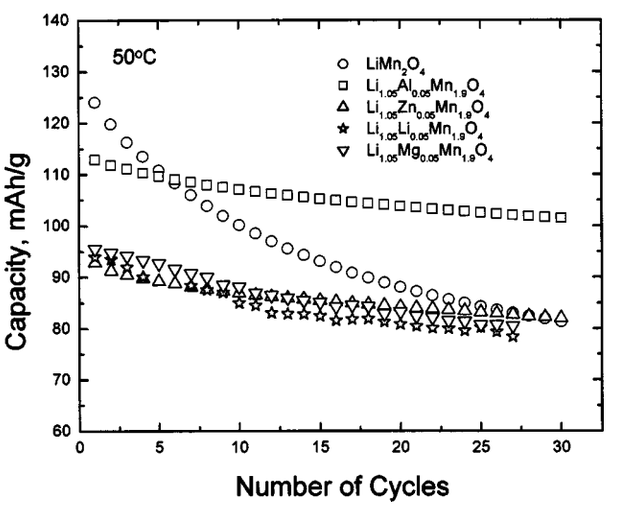

Figure 5. Capacity *vs.* cycle number plots recorded at 50°C for substituted $Li_{1.05}M_{0.05}Mn_{1.90}O_4$ spinel electrodes (M = Li, Mg, Al, Zn) compared with a standard $LiMn_2O_4$ electrode for cycles 1-30.

Zn, or Al ions that remain on the tetrahedral sites of the spinel electrode, particularly toward the top of charge, thereby suppressing the diffusion of manganese ions into the 8a-16c-8a-16c- pathway and subsequent manganese dissolution at the electrode surface. Note that when cells operate at 50°C and reach 100 cycles, the rate of capacity fade of the standard $LiMn_2O_4$ electrode parallels that of the Zn- and Al-substituted electrodes (Fig. 6). One explanation for this behavior is that, on long-term cycling, the dissolution of manganese from the $LiMn_2O_4$ electrode ultimately yields a lithium-rich spinel, at least at the electrode surface, thereby stabilizing the electrode and mimicking the behavior of a lithium-rich $Li_{1+x}Mn_{2-x}O_4$ electrode.

From a crystallographic viewpoint, it is possible to speculate how Mn dissolution is suppressed at the electrode surface. Reaction 1 shows that two Mn^{3+} ions are required to effect the disproportionation reaction, one which is oxidized to Mn^{4+}, the other reduced to Mn^{2+}. It is well known that such disproportionation reactions are accompanied by the migration of at least one of the two ions and that these reactions can occur within a crystal lattice during the electrochemical extraction of lithium. For example, during lithium extraction from layered $LiVO_2$ (space group $R3m$),[33] the oxidized V^{4+} ions disproportionate into V^{5+} and V^{3+} ions at a critical composition $Li_{1-x}VO_2$ ($x = 0.3$) and potential according to the reaction

$$2V^{4+}_{(oct)} \rightarrow V^{5+}_{(tet)} + V^{3+}_{(oct)} \quad [2]$$

During this reaction, the vanadium ions migrate from the octahedral 3a sites of the vanadium-rich layer into the octahedral 3b sites of the lithium-rich layer via a 6c tetrahedron in which the vanadium ions adopt an intermediate pentavalent state;[33] the end product is a defect rocksalt structure in which $V^{4+/3+}$ ions occupy octahedral sites in alternate layers. By contrast, during lithium extraction of lithium from layered $LiMnO_2$, it is the Mn^{3+} ions that disproportionate by a similar mechanism but, in this instance, the manganese ions adopt an intermediate divalent state in the tetrahedral sites during their migration from one layer to the next to yield a spinel-like framework that contains $Mn^{4+/3+}$ ions[20]

$$2Mn^{3+}_{(oct)} \rightarrow Mn^{2+}_{(tet)} + Mn^{4+}_{(oct)} \quad [3]$$

The intermediate 6c tetrahedral sites are temporarily occupied during the phase transitions; these sites are energetically unfavorable because each tetrahedron in a layered $LiMO_2$ structure shares three of its faces with neighboring occupied M octahedra.

It has also been demonstrated that lithium extraction from the spinel $Li[V_2]O_4$ (space group $Fd3m$) is accompanied, at a critical composition $Li_{1-x}[V_2]O_4$ ($x \sim 0.3$) and potential, by the migration of vanadium ions from an octahedral 16d site, through a face-shared tetrahedron (probably a 48f site which is energetically more favorable than an 8b site) into an octahedral 16c site to yield a defect rocksalt structure similar to delithiated $Li_{1-x}VO_2$.[34] This reaction occurs despite the fact that each 48f tetrahedron in the spinel structure shares two of its faces with neighboring 16d octahedra that are occupied by transition metal ions.

Using the argument above, it therefore seems plausible that, during the acid attack of $LiMn_2O_4$ electrodes, which drives the disproportionation reaction at the crystal surface, the manganese ions would migrate from an octahedral 16d site through a tetrahedral 48f site in which it adopts a divalent state, and thereby into the 8a-16c-8a-16c-network of the spinel structure, each 16c octahedron sharing six of its eight faces with neighboring 48f tetrahedra.

It should be borne in mind that dissolution of manganese from $LiMn_2O_4$ is accompanied by the loss of lithium and oxygen according to the reaction

$$2LiMn_2O_4 \rightarrow 3\lambda\text{-}MnO_2 + MnO + Li_2O \qquad [4]$$

Reaction 4 suggests that the migration of the manganese ions from the 16d sites and the dissolution of MnO and Li_2O from the structure take place simultaneously and that the Li ions (and the oxygen ions with which they are associated) are dissolved from the proximity of the 8a-16c-8a-16c-channels. From pH and steric viewpoints, any residual (surplus) ions, particularly those ions forming acid-resistant oxides, occupying tetrahedral 8a sites at the surface of highly delithiated spinel electrodes may be expected to lower the surface potential, retard the disproportionation reaction, block Mn diffusion from the 16d sites and slow the dissolution process.

The lithium-substituted spinels, $Li_{1+x}Mn_{2-x}O_4$, may seem ideal for stabilizing $LiMn_2O_4$ spinel electrodes because lithium substitution for manganese does not disturb the Li^+-ion diffusion in the 3-D 8a-16c-8a-16c- network of face-shared tetrahedra and octahedra in the spinel structure. However, because lithium is so mobile within the interstitial space of the spinel framework, it may not be as effective as a multivalent substituent cation such as trivalent Al (which is not as mobile as lithium) in blocking Mn diffusion into neighboring tetrahedral sites at high potentials ($\sim$4 V) at the electrode surface and in suppressing Mn dissolution into the electrolyte. If the Al ions had occupied the octahedral B sites at a 2.5% level (rather than the tetrahedral sites at a 5% level), *i.e.,* with only Li in the 8a-16c-8a-16c- network, then our hypothesis is that the electrochemical cycling stability of Al-substituted spinel electrodes would not have been so significantly different to Li-substituted electrodes. The same argument holds for Zn- and Mg-substituted electrodes. The significantly lower solubility of aluminum oxides in acidic media compared to Li_2O, as well as the recent interest in Al-substituted spinel electrodes by the lithium battery industry, lend support to this hypothesis.

Conclusions

This study has demonstrated that the presence of residual, substituent ions in the tetrahedral A sites at the surface of substituted spinel $LiM_xMn_{2-x}O_4$ electrodes may play a critical role in the stabilization of the electrodes at room temperature as well as at 50°C. However, increasing the amount of residual cations in these sites at the top of charge compromises the capacity of the electrode. Although low concentrations of stabilizing M cations can make a significant contribution to improving the stability of spinel electrodes, it is likely that this procedure will have to be coupled with alternative approaches, *e.g.,* coating techniques or the use of non-fluorinated electrolyte salts to totally overcome manganese dissolution and the capacity loss effects of $LiMn_2O_4$ spinel electrodes in lithium-ion cells with carbon negative electrodes.

Acknowledgments

We wish to thank Simine Short of the Materials Science Division at Argonne National Laboratory for collecting the neutron diffraction data at IPNS. Support for this work from the Office of Basic Energy Sciences, Division of Chemical Sciences, and the Office of Advanced Automotive Technologies, both of the U.S. Department of Energy, under contract no. W-31-109-Eng-38, is gratefully acknowledged.

Argonne National Laboratory assisted in meeting the publication costs of this article.

References

1. M. M. Thackeray, W. I. F. David, and J. B. Goodenough, *Mater. Res. Bull.*, **17**, 785 (1982).
2. M. M. Thackeray, W. I. F. David, P. G. Bruce, and J. B. Goodenough, *Mater. Res. Bull.*, **18**, 461 (1983).
3. M. M. Thackeray, P. J. Johnson, L. A. de Picciotto, P. G. Bruce, and J. B. Goodenough, *Mater. Res. Bull.*, **19**, 179-187 (1984).
4. K. M. Colbow, J. R. Dahn, and R. R. Haering, *J. Power Sources*, **26**, 397 (1989).
5. M. M. Thackeray, *Handbook of Battery Materials*, J. O. Besenhard, Editor, p. 293, Wiley-VCH, Weinheim, Germany (1999).
6. T. Ohzuku, M. Kitagawa, and T. Hirai, *J. Electrochem. Soc.*, **137**, 769 (1990).
7. J. M. Tarascon, E. Wang, F. K. Shokoohi, W. R. McKinnon, and S. Colson, *J. Electrochem. Soc.*, **138**, 2859 (1991).
8. R. J. Gummow, A. de Kock, and M. M. Thackeray, *Solid State Ionics*, **69**, 59 (1994).
9. G. Amatucci and J.-M. Tarascon, *J. Electrochem. Soc.*, **149**, K31 (2002).
10. Q. Zhong, A. Bonakdarpour, M. Zhang, Y. Gao, and J. R. Dahn, *J. Electrochem. Soc.*, **144**, 205 (1997).
11. Y. Ein-Eli, S. H. Lu, M. A. Rzeznik, S. Mukerjee, X. Q. Yang, and J. McBreen, *J. Electrochem. Soc.*, **145**, 3383 (1998).
12. D. Song, H. Ikuta, T. Uchida, and M. Wakihara, *Solid State Ionics*, **117**, 151 (1999).
13. S.-K. Myung, S. Komaba, and N. Kumagai, *J. Electrochem. Soc.*, **148**, A482 (2001).
14. G. G. Amatucci, A. Blyr, C. Sigala, P. Alfonse, and J. M. Tarascon, *Solid State Ionics*, **104**, 13 (1997).
15. C. S. Johnson, K. Lauzze, D. Abraham, N. Dietz, M. Thackeray, W. Zeltner, and M. Anderson, IBA-HBC2003, Proceedings Abstracts of the Ernest Yeager Memorial Symposium, the International Battery Association, and the Hawaii Battery Conference, Jan 7-10, 2003.
16. K. Xu, S. Zhang, T. R. Jow, W. Xu, and C. A. Austen, *Electrochem. Solid-State Lett.*, **5**, A26 (2002).
17. J. Liu, K. Xu, T. R. Jow, and K. Amine, Abstract 135, The Electrochemical Society Meeting Abstracts, PV 2002-2, Salt Lake City, Utah, Oct 20-25, 2002.
18. A. Larson and R. B. von Dreele, *GSAS: General Structure Analysis System*, LANSCE, Los Alamos, NM (1985).
19. M. M. Thackeray, P. J. Johnson, L. A. de Picciotto, P. G. Bruce, and J. B. Goodenough, *Mater. Res. Bull.*, **19**, 179 (1984).
20. J. Reed, G. Ceder, and A. Van der Ven, *Electrochem. Solid-State Lett.*, **4**, A78 (2001).
21. Y. J. Lee, S.-H. Park, C. Eng, J. B. Parise, and C. P. Grey, *Chem. Mater.*, **14**, 194 (2002).
22. R. J. Hill, J. R. Craig, and G. V. Gibbs, *Phys. Chem. Miner.*, **4**, 317 (1979).
23. H. Shigamura, M. Tabuchi, H. Kobayashi, H. Sakaebe, A. Hirano, and H. Kageyama, *J. Mater. Chem.*, **12**, 1882 (2002).
24. H. Berg, J. O. Thomas, W. Liu, and G. Farrington, *Solid State Ionics*, **112**, 165 (1998).
25. D. Capsoni, M. Bini, G. Chiodelli, P. Mustarelli, V. Massorotti, C. B. Azzoni, M. C. Mozzati, and L. Linati, *J. Phys. Chem.*, **106**, 7432 (2002).
26. S. Komaba, K. Oikawa, S-T. Myung, N. Kumagai, and T. Kamiyama, *Solid State Ionics*, **149**, 47 (2002).
27. J. A. Dean, *Lange's Handbook of Chemistry*, 15th ed., p. 4.30, McGraw-Hill, New York (1999).
28. J. B. Goodenough, M. M. Thackeray, W. I. F. David, and P. G. Bruce, *Rev. Chim. Miner.*, **21**, 435-455 (1984).
29. H. Bjork, T. Gustafsson, and J. O. Thomas, *Electrochem. Commun.*, **3**, 187 (2001).
30. Y. Xia and M. Yoshio, *J. Electrochem. Soc.*, **144**, 4186 (1997).
31. Y. Shin and A. Manthiram, *Electrochem. Solid-State Lett.*, **6**, A34 (2003).
32. G. Amatucci and J.-M. Tarascon, *J. Electrochem. Soc.*, **149**, K31 (2002).
33. L. A. de Picciotto, M. M. Thackeray, W. I. F. David, P. G. Bruce, and J. B. Goodenough, *Mater. Res. Bull.*, **19**, 1497 (1984).
34. L. A. de Picciotto and M. M. Thackeray, *Solid State Ionics*, **18,19**, 773 (1986).